Automotive Experiences
Vol. 4 No.1 (2021) pp. 27-35
p-ISSN: 2615-6202 e-ISSN: 2615-6636

Research Paper

Effect of Magnetic Field Induce Arc in Autogenous TIG Welding of 304 Stainless Steel Butt Joint

Haikal[1], Moch.Chamim[2], Deni Andriyansyah[3], Emanuel Budi Raharjo[4], Ario Sunar Baskoro [5], Isnarno[6]

[1,2,3]Department of Mechanical Engineering, Sekolah Tinggi Teknologi Warga Surakarta, 57552, Indonesia
[4]Department of Electrical Engineering, Sekolah Tinggi Teknologi Warga Surakarta, 57552, Indonesia
[5]Department of Mechanical Engineering, Universitas Indonesia, 16424, Indonesia
[6]Department of Civil Engineering, Universitas Tunas Pembangunan, 57139, Indonesia

haikal@sttw.ac.id

https://doi.org/10.31603/ae.4199

Published by Automotive Laboratory of Universitas Muhammadiyah Magelang collaboration with Association of Indonesian Vocational Educators (AIVE)

Article Info
Submitted:
05/11/2020
Revised:
21/11/2020
Accepted:
22/11/2020
Online first:
05/02/2021

Abstract

This paper reports the use of External Magnetic Field-Tungsten Inert Gas (EMF-TIG) method in butt joint applications to determine the effect of welding arc compression on the quality of butt joint of SS 304 thin plate was reported. The welding process was performed without using filler or autogenous welds. The external magnetic field was generated by placing a magnetic solenoid around the TIG welding torch. The results of this study showed that EMF-TIG welding can produce a more uniform bead width along the weld line compare with conventional TIG. Moreover, the D/W ratio obtained under external magnetic field was higher than without magnetic. However, the tensile strength of butt joint decreased with EMF-TIG because there is constriction in arc welding which produces shrinkage weld pool volume. In addition, high welding speeds result in a decrease in the tensile strength of both conventional TIG and EMF-TIG welds.

Keywords: EMF-TIG; Butt joint; Autogenous; Stainless Steel 304; Arc welding

Abstrak

Makalah ini melaporkan penggunaan metode External Magnetic Field-Tungsten Inert Gas (EMF-TIG) dalam aplikasi sambungan butt untuk mengetahui pengaruh kompresi busur pengelasan terhadap kualitas sambungan butt pelat tipis SS 304. Proses pengelasan dilakukan tanpa menggunakan filler atau autogenous weld. Medan magnet eksternal dihasilkan dengan menempatkan solenoid magnet di sekitar torch las TIG. Hasil penelitian ini menunjukkan bahwa pengelasan EMF-TIG dapat menghasilkan lebar bead yang lebih seragam di sepanjang garis las dibandingkan dengan TIG konvensional. Selain itu, rasio D/W yang diperoleh di bawah medan magnet eksternal lebih tinggi daripada tanpa magnet. Namun kekuatan tarik sambungan butt menurun dengan EMF-TIG karena adanya penyempitan pada pengelasan busur yang menghasilkan penyusutan volume pool las. Selain itu, kecepatan pengelasan yang tinggi menghasilkan penurunan kekuatan tarik dari pengelasan TIG dan EMF-TIG konvensional.

Kata-kata kunci: *EMF-TIG; Butt joint; Autogenous; Stainless Steel 304; Busur las*

1. Introduction

Tungsten Inert Gas (TIG) welding is an arc welding with wide industrial use because it can join different materials. For instance, it may join similar or dissimilar metal materials with high-quality joints. The fusion of weld metals is attributed to welding arc heat between the non-consumable tungsten electrode and specimen during welding. The welding arc area is protected from the atmosphere by the inactive shielding gas, such as helium and argon, that flow through the

torch nozzle. TIG welding can be operated without used filler metals, hence called autogenous welding [1]. This approach was used to join thin material with thicknesses of 3 mm or less [,]. In comparison, filler metals were used when the materials have a thickness of more than 3 mm. Generally, edge preparation is conducted to joint, thick material, while multi passes with filler metals fill the groove joints.

Deep penetration is an essential factor that defines the quality of the weld joint. The increasing deep penetration during the TIG welding process can be obtained by raising the welding current. However, welding defects, such as distortion, can be increased with incremental welding current. This is because of the high heat input in the welding area [4]. Austenitic stainless steel has the highest thermal expansion than the others. However, it has the lowest thermal conductivity than carbon and allows steel. Since this material is very susceptible, it is often distorted after welding. According to Tseng [5], welding 316L stainless steel using conventional TIG welding leads to increased angular distortion. Apart from currents, plate thickness also affects distortion. Okano and Mochizuki's previous study showed that the distortion due to current decreased with increasing thickness of the welded plate [6].

Previous studies have widely practiced the engineering of the welding process to increase the depth of weld penetration. This included EMF-TIG (External Magnetic Field Tungsten Inert Gas), a conventional TIG welding method supplemented by an external magnetic field effect. The shape behavior of the welding arc can be altered depending on the configuration of the welding's external magnetic field [7-9]. Based on a variety of configurations, EMF can be categorized as CMF (Cups Magnetic Field), AMF (Axial Magnetic Field), LMF (Longitudinal Magnetic Field), TMF (Transverse Magnetic Field), and RMF (Rotating Magnetic Field) [10]. Nomura et al. [11] stated that the welding arc could be controlled using an external magnetic field, leading to a deeper weld penetration than conventional TIG welding. Shoichi et al. [12] examined the effect of EMF on TIG welding with filler for 2 welding positions of 1 G and 4 G. The results showed that the use of an external magnetic field with a certain position leads to a force in the direction of gravity or made against it (antigravity) to reduce the impact of welding defects, such as undercut. Baskoro et al. [13] examined TIG welding using a dynamic magnetic field. The results showed that the magnetic field generated by the solenoid dynamically leads to a deeper weld penetration. Applications of AC and DC magnetic fields can also improve weld quality on aluminum and stainless steel material for high power laser beam [14-16].

According to studies, the use of external magnetic fields in conventional TIG welds may increase the depth of weld penetration and reduce the impact of welding defects. Metallurgical and mechanical properties of 304L steel in TIG welding under the application of a permanent external magnetic field for butt joint applications has also been studied recently [17]. However, there is no literature on using the EMF-TIG with dynamic activation method for butt joint application. This experiment is necessary because the butt joint method in welding is widely used. This study examines the effect of the addition of dynamic external magnetic field to the quality of weld joint results of AISI 304 thin plate with a butt-joint method. AISI 304 is a non-magnetic still that does not affect the presence of a magnetic field. However, the external magnetic field is applied to influence the arc's shape, which might affect the resulting weld pool's dimensions. This has been proven by several studies using stainless steel as specimen joints that were non-magnetic. The influence of process parameters on the surface appearance, weld geometry, and tensile strength have been studied systematically.

2. Materials and Methods

In this experiment, AISI 304 stainless steel of 3 mm thickness was chosen. The plate materials were cut into pieces of 110 x 70 mm while the specimens were joined as butt joints method. The welding experiment was conducted using a GeKaMac power TIG 2200 DC pulse welding machine. **Figure 1** shows the schematic of the experimental apparatus. Single-pass of autogenous TIG welds were made along the centerline of the butt joint specimen with and without the use of an external magnetic field. **Table 1** shows the chemical composition of the stainless steel used. Before welding, all samples'

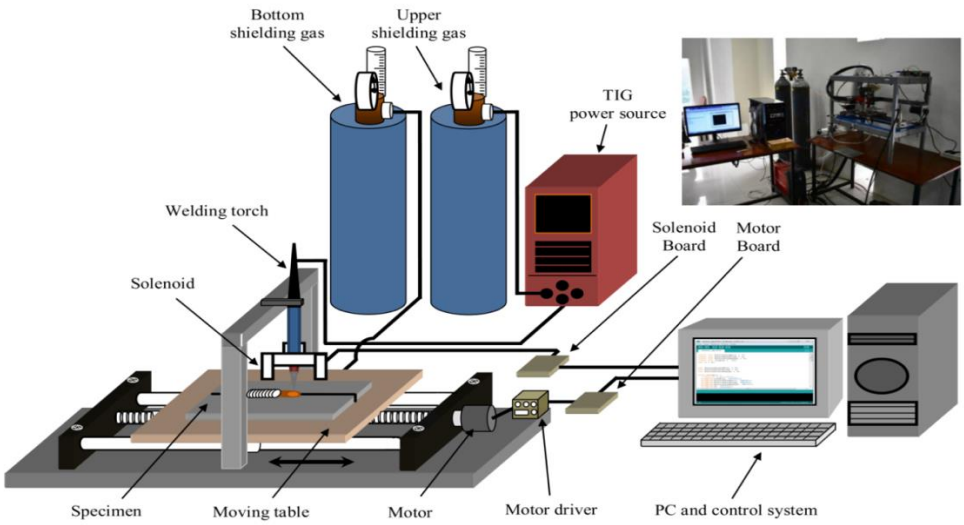

Figure 1. Schematic of EMF-TIG welding apparatus [18]

Table 1. Chemical composition of sheet materials (wt%)

	C	Si	Mn	P	S	Ni	Cr
SUS 304	< 0.07	< 0.75	< 2.00	< 0.045	< 0.030	8.00 ~ 10.50	17.50 ~ 19.50

surfaces were cleaned by 400 grit flexible abrasive papers and cleaned chemically with acetone solution to remove surface impurities. **Table 2** shows the welding conditions and parameters of the process that were used in this experiment. Three sample butt-weld specimens were performed per welding condition, including for the visualization and tensile tests. This was followed by one sample without joint with a thickness of 5 mm for metallographic observation.

During welding, a dynamic external magnetic field was generated by a solenoid and activated using a microcontroller. Solenoids were arranged around on the torch with configurations of the magnetic field like cusp, as shown in **Figure 2**. The lateral and vertical distance from the solenoid to the specimen's top surface is 5 mm and 50 mm, respectively. This helps obtain the maximum magnetic flux density in the weld pool area.

The top bead's visualization test and back bead width along the weld line are measured using the caliper with a measurement distance of 10 cm for all welded specimens. samples of weld with and without EMF-TIG were prepared according to ASTM E8 / E8M standards to determine the tensile load of TIG welding specimens. The tensile tests were performed using the RTF-2350 Universal Testing Machine at a constant cross-head velocity of 5 mm/min.

The cross-section of the weld specimens was cut using a band-saw machine for macrostructure observation. All the macrostructure specimens were prepared by grinding and polishing with abrasive paper 220-2000 grit. This was followed by electro etching (6-8 volt during 90 s) with oxalate solution (15gr $C_2H_2O_4'2H_2O$ + 100 ml aquades) to reveal the weld pool shape.

Table 2. Welding conditions used in the experiment

Parameter	Unit	Value
Power source	Dimensionless	DCEN
Welding current	A	100 - 110
Welding speed	mm/sec	1.6 - 2.0
AWS classification	Dimensionless	E W Th-2
Electrode diameter	mm	2.4
Nominal arc length	mm	2
Shielding gas	Dimensionless	99,99% Argon
Upper Shielding gas flow rate	L/min	10
Bottom Shielding gas flow rate	L/min	5

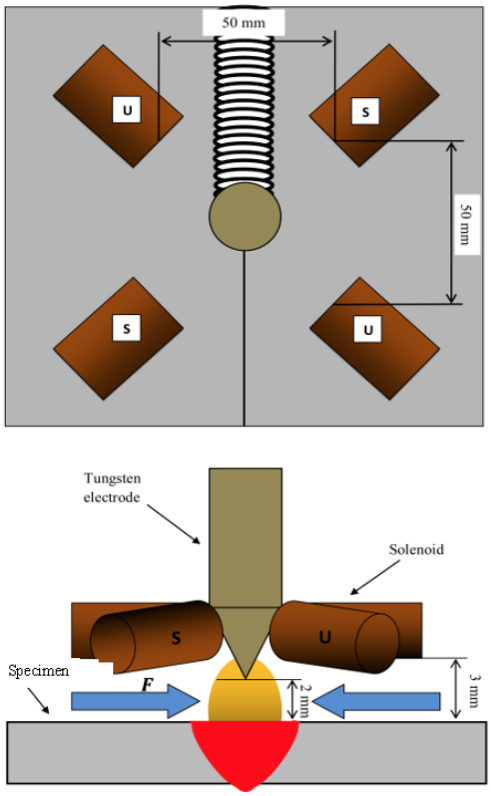

Figure 2. Arrangement of solenoids around welding torch

3. Result and Discussion

3.1. Visualization test on conventional TIG welds

The current and welding speed significantly affect the geometry of TIG welding. This study showed that increasing weld time affects the decrease in the top bead. Furthermore, increased welding current also affects the increase in the upper weld bead's width, as shown in **Figure 3**. This is in line with Aval et al. [19], which stated that heat input decreases with increasing welding speed, reducing the weld pool volume.

The increase in weld speed has a significant influence on the weld bead width than the current rise. This is in line with the formula for finding a large heat input, which is $Hin = \eta E I / V$. The higher the welding speed, the lower the heat input. Increased welding current can also increase the electromagnetic forces. This force pushes the melted metal downward to make the weld pool deeper during the welding process [1].

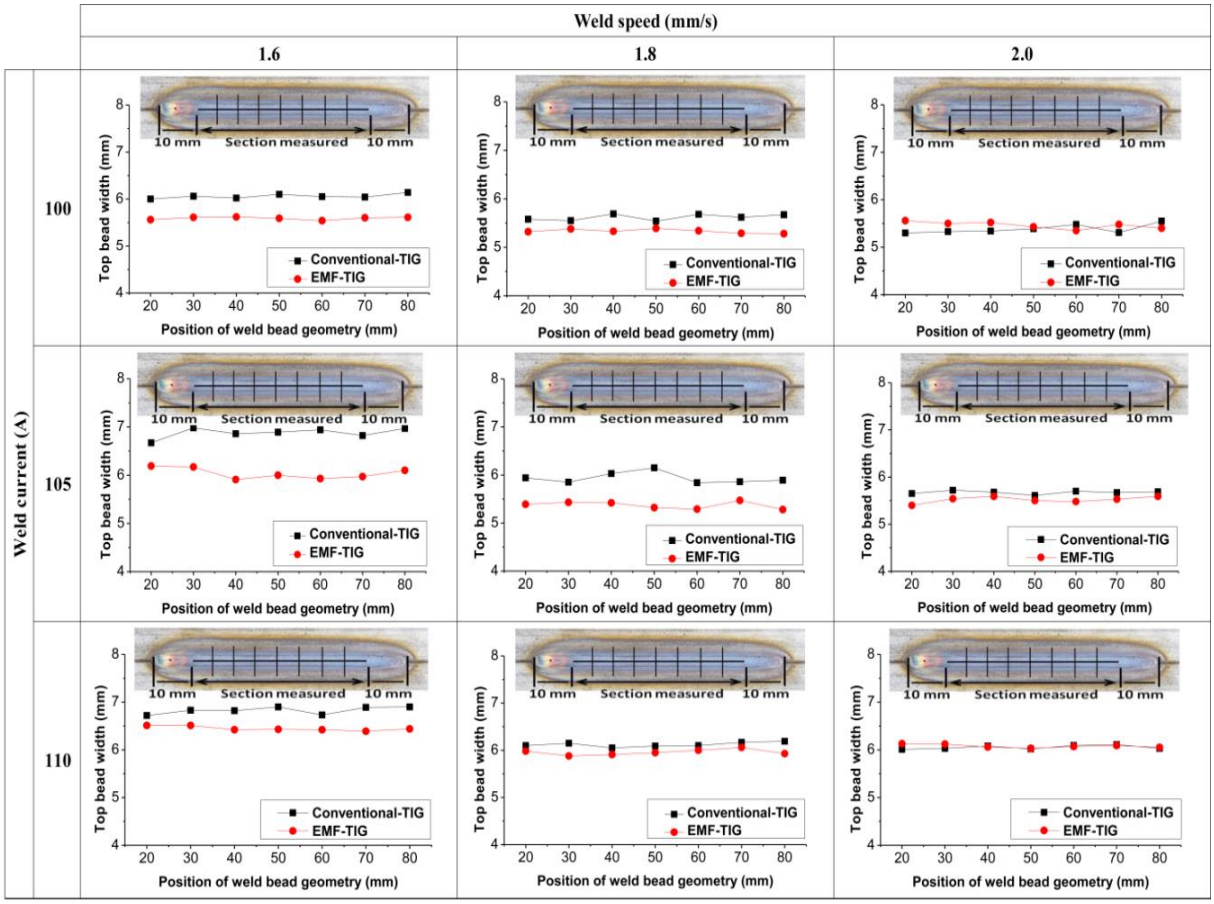

Figure 3. Comparing the weld bead width in butt joint for all parameters.

Table 3 shows the comparison between the weld bead width on the welding process with or without an external magnetic field. In conventional TIG welding, currents of 100 A and 105 A inclined to produce uniform weld bead widths along the weld line. Otherwise, the weld bead width is more uniform when using the current 110 A. This occurred because the use of low current is very susceptible to the occurrence of arc welding deflection [13].

3.2. *Comparison of bead width on TIG welding with and without external magnetic field*

The external magnetic field, which is activated dynamically and arranged in a complex form, compresses the welding arc. This is evidenced by the decrease of weld bead width above the EMF TIG than the conventional TIG welding, as shown in Figure 3. However, the external magnetic field's ability to compress the welding arc decreases with increasing welding speed, as shown in Table 3.

Figure 4 shows the scheme of forming a plasma arc during welding with or without an external magnetic field. Figure 4(a) shows the presence of an internal magnetic field formed in a counter-clockwise movement during the conventional TIG DCEN polarity welding [11]. Arc welding using DCEN and DCEP polarity leads to different weld depths. Previous studies proved that a simulation of TIG welding using DCEP polarity leads to a lower welding arc temperature than DCEN polarity, hence the penetration of the weld bead is narrow [20]. The encounter between the weld current and the internal magnetic field produces an electromagnetic force that leads to the center axis of the arc. The addition of an external magnetic field produces a larger electromagnetic force. The welding arc can be compressed, as shown in Figure 4(b).

Table 3. The top bead width of conventional and EMF-TIG welds

Weld current (A)	Travel Speed (mm/s)	Conventional TIG		EMF-TIG	
		Top bead width (mm)	Deviation (mm)	Top bead width (mm)	Deviation (mm)
100	1.6	6.06	0.05	5.59	0.03
100	1.8	5.62	0.06	5.53	0.04
100	2.05	5.39	0.10	5.46	0.07
105	1.6	6.88	0.11	6.04	0.11
105	1.8	5.94	0.11	5.37	0.07
105	2.05	5.67	0.04	5.52	0.07
110	1.6	6.83	0.08	6.54	0.05
110	1.8	6.12	0.05	5.96	0.06
110	2.05	6.05	0.04	6.08	0.04

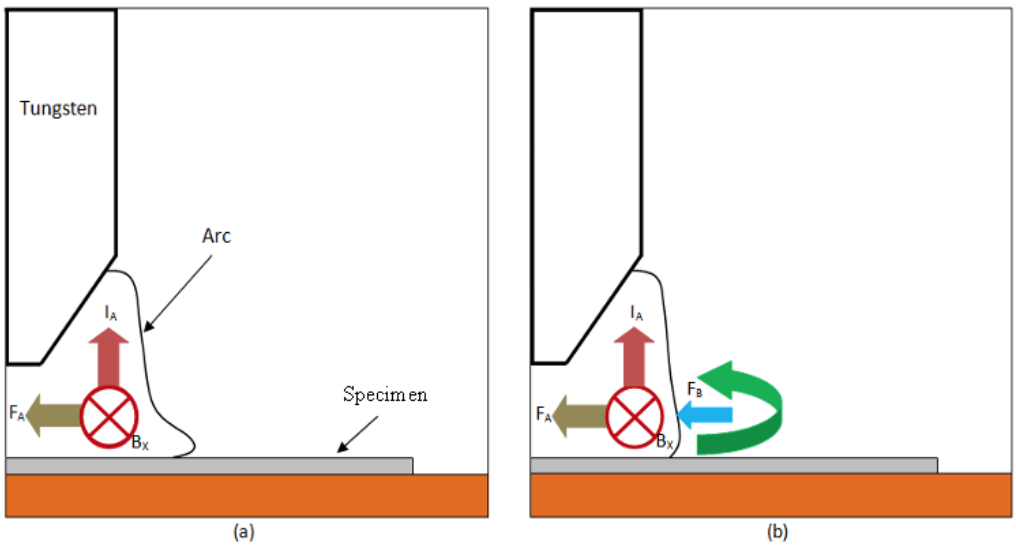

Figure 4. Schematic of arc welding during the welding process: (a). Conventional-TIG and (b). EMF-TIG

The top bead width for speed 2 mm/s has a wider size than 1.6 and 1.8 mm/s. This is because the external magnetic field's ability to compress the welding arc decreases when the welding speed is high. The welding parameters with 105 A currents have a greater compression effect than 110 A. This is because the magnitude of the welding current greatly influences the welding arc's stiffness. For instance, it can be increased by raising the welding current, reducing the EMF's impact on the welding arc [13].

3.3. *The geometric shape of Conventional and EMF-TIG welds*

Figure 5 shows the macro photographs of conventional TIG-welded specimens at a current of 105-110 A with a travel speed of 1.6 mm/s. The increase in welding current affects the depth of the weld penetration. This is because of higher heat input and the pressure force that drives the fluid flow in the weld pool. The magnitude of heat input during welding is 0.656 kJ/mm, 0.613 kJ/mm, and 0.578 kJ/mm. According to previous studies, the TIG welding, both autogenous and non-autogenous welding, has 4 driving forces for fluid flow, including buoyancy, Lorentz, Marangoni, and shear stress pool surface by the arc plasma [1]. When the current is increased, the Lorentz force generated also increases. When the base metal melts along the pool axis, the Lorentz force is produced due to the perpendicular confluence between the arc current and the magnetic field, pushing the liquid downward along the pool axis and deepens the weld pool [19].

The welding process with a magnetic field produces a narrower welding bead shape and deeper penetration. The narrowing of the weld bead width is attributed to external Lorentz force that shrinks the radius of the welding arc Therefore, the heat generated by the welding arc increases. The top bead width using an external magnetic field led to a decrease of 8.0%, 6.7%, and 3.2%, respectively.

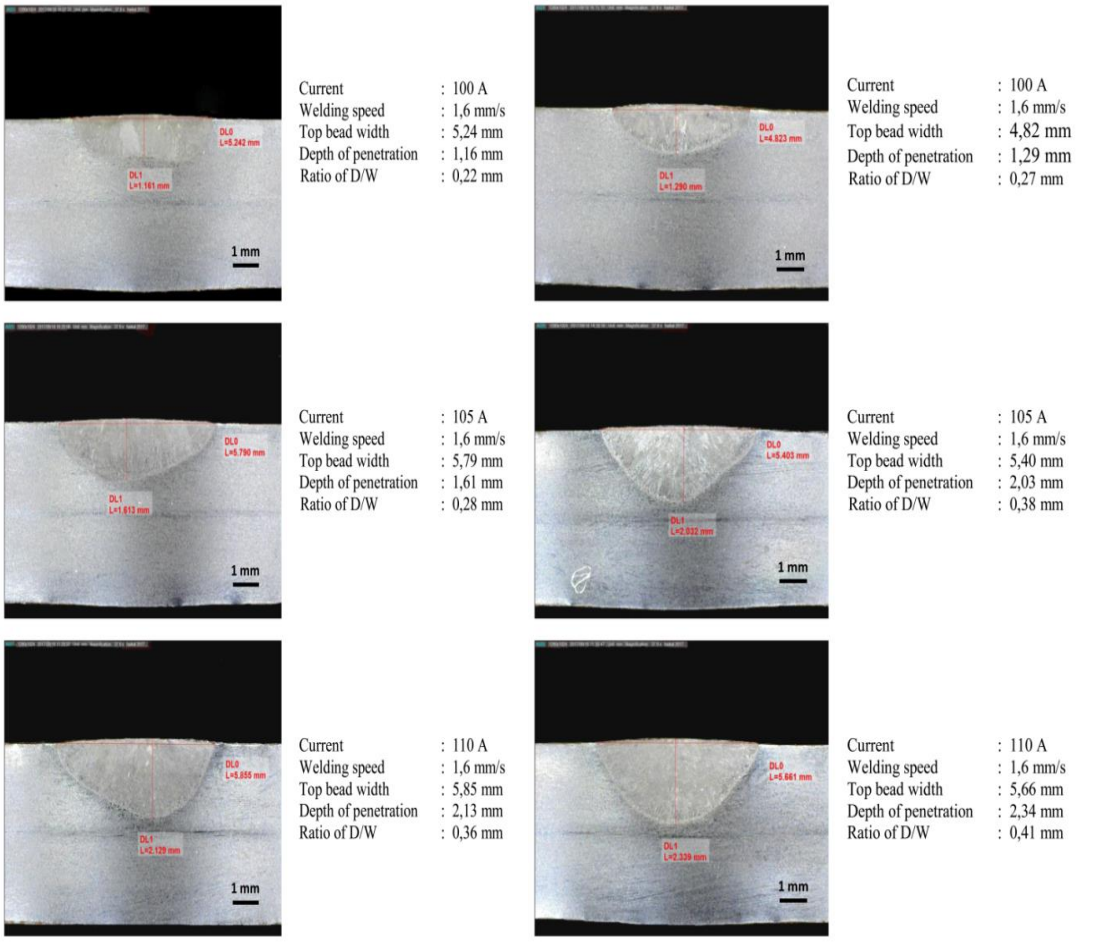

Figure 5. The geometric shape of (a) Conventional TIG welding and (b) EMF-TIG welding.

The weld penetration depths with an external magnetic field led to an increase of 11.2%, 26.1%, and 9.8%. The external magnetic field's ability to increase the depth of the weld decreases when the current used in the welding process is 110 A. This is because the heat input generated is too large, decreasing the capability of EMF to compression of the welding arc. **Figure 6** shows the weld bead width ratio with the penetration depth specimens at a current of 105-110 A with a travel speed of 1.6 mm/s. The increasing welding current increases the D/W ratio, both in the Conventional TIG and EMF-TIG welding. The D / W ratio was increased using the EMF-TIG welding method because the resulting penetration was deeper while the upper bead's width decreased. This is in line with Nomura et al. [21]. The highest D/W ratio was reported under EMF-TIG than conventional TIG in welding currents of 105 A.

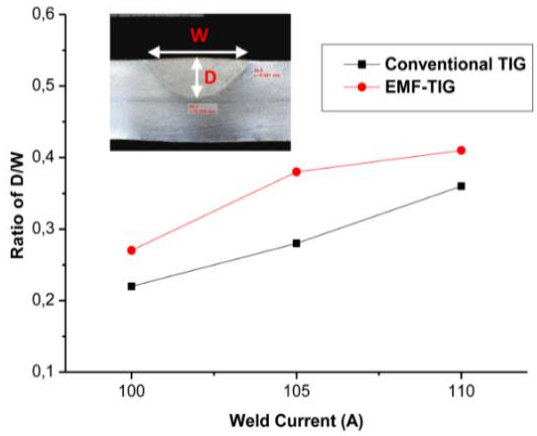

Figure 6. The weld bead width ratio with the penetration depth (D/W) of the weld pool in Conventional TIG and EMF-TIG welding

3.4. Tensile test

Tensile testing was conducted to determine the quality of welding results with the welding parameters determined. The weld joint's tensile strength at a speed of 1.6 mm/s, 1.8 mm/s, and 2.0 mm/s with a welding current of 105 A had 503.39 MPa, 509.94 MPa, and 454.72 MPa, respectively. The EMF-TIG method had 461.99 MPa, 465.16 MPa, and 398.80 MPa. The tensile strength of welded materials decreased when the welding speed was too high, as shown in Figure 7. This is in line with (Aval et al. [19]), which stated that the most significant effect of welding speed is its influence on the weld pool's volume. With the increase in welding speed, the amount of heat input decreases, reducing the weld pool volume.

The decrease in the strength of the welded joint due to the decrease in the weld pool volume indicated by the width of the upper weld bead is narrower, shown in **Figure 3**. However, when the welding speed is 1.8 mm/s, the tensile strength is slightly increased compared to 1.6 mm/s in both conventional welding and EMF-TIG methods. This is because the welding method used in this study does not utilize filler to fill gaps except for a parent metal. When the welding speed is too low, high heat input is obtained high and lengthening the cooling process. Therefore, the melted metal falls for the weld pool area to shrink. This is corroborated by previous studies, which stated that welding with high heat input conditions leads to a molten sag down and an undercut [12].

The tensile strength produced by welding with an external magnetic field is lower than conventional TIG welding on thin-plate welding joints application without filler. The welded joint's strength using no filler is greatly influenced by how much the parent material is melting. However, the ratio of D/W produced by EMF-TIG welding is greater than that of conventional TIG (Figure 6). The width of the weld bead experiences a significant narrowing. When applied to welding thin plates without filler, the volume of the weld pool is reduced. This is because the external magnetic field's electromagnetic force led to a compressed arc welding area. The resulting parent material melt, hence the strength of the welded joints decreases.

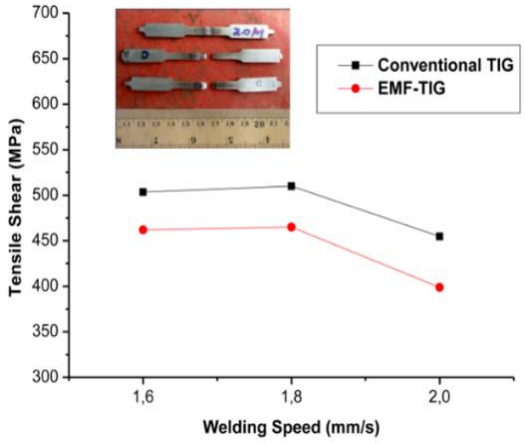

Figure 7. The effect of weld speed on tensile strength of weld joints with and without external magnetic field

4. Conclusion

This study makes the following conclusions:

1. EMF-TIG with dynamic activation produces a more uniform bead width along the weld line in the butt joint than the conventional TIG welding. In conventional TIG, the use of low current is very susceptible to arc welding deflection. When there is an additional magnetic field around the welding arc area, external electromagnetic forces hold the arc in position.
2. The weld area's microstructure showed that a narrower welding bead shape and the deeper weld penetration are produced using an additional magnetic field. Weld penetration depths at currents of 100 A, 105 A, and 110 using an external magnetic field increase by 11.2%, 26.1%, and 9.8%, respectively. Furthermore, the highest D/W ratio reported under EMF-TIG than the Conventional TIG was in welding currents of 105 A.
3. The weld joint's tensile strength at a speed of 1.6 mm/s, 1.8 mm/s, and 2.0 mm/s with a welding current of 105 A leads to 503.39 MPa, 509.94 MPa, and 454.72 MPa, respectively. In comparison, the EMF-TIG method produces 461.99 MPa, 465.16 MPa, and 398.80 MPa, respectively. The tensile strength of welded materials decreases with EMF-TIG due to the shrinking of weld pool volume. The weld bead's width experiences a significant narrowing, reducing the weld pool's volume when applied to thin welding plates without filler.
4. With increasing weld speed, the tensile strength decreased. However, the tensile strength value at a welding speed of 1.8 mm/s is higher than 1.6 mm/s due to a molten sag down affected by high input energy at a lower speed.

Acknowledgment

The author expresses gratitude to the Directorate Research and Public Service, Universitas Indonesia through the contract number 1753/UN2.R12/PPM.00.00/2016 and the Institute for Research and Community Service, Sekolah Tinggi Teknologi Warga Surakarta.

Author's Declaration

Authors' contributions and responsibilities

The authors made substantial contributions to the study's conception and design, including taking responsibility for data analysis, interpretation, and discussion of the results. The final manuscript was read and approved.

Funding

This research was funded by the Sekolah Tinggi Teknologi Warga Surakarta, Universitas Indonesia, and Universitas Tunas Pembangunan.

Availability of data and materials

All data are available from the authors.

Competing interests

The authors declare no competing interest.

Additional information

No additional information from the authors.

References

[1] H. Eisazadeh, D. J. Haines, and M. Torabizadeh, "Effects of gravity on mechanical properties of GTA welded joints," *Journal of Materials Processing Technology*, vol. 214, pp. 1136-1142, 2014.

[2] K.-H. Tseng and K.-L. Chen, "Comparisons between TiO_2- and SiO_2-flux assisted TIG welding processes," *Journal of Nanoscience and Nanotechnology*, vol. 12, pp. 6359-6367, 2012.

[3] K.-H. Tseng and K.-J. Chuang, "Application of iron-based powders in tungsten inert gas welding for 17Cr–10Ni–2Mo alloys," *Powder Technology*, vol. 228, pp. 36-46, 2012.

[4] S. Okano and M. Mochizuki, "Transient distortion behavior during TIG welding of thin steel plate," *Journal of Materials Processing Technology*, vol. 241, pp. 103-111, 2017.

[5] K.-H. Tseng, "Development and application of oxide-based flux powder for tungsten inert gas welding of austenitic stainless steels," *Powder Technology*, vol. 233, pp. 72-79, 2013.

[6] S. Okano and M. Mochizuki, "Experimental study on generation characteristics of weld buckling distortion in thin plate," *Transactions of the JSME (in Japanese)*, vol. 82, pp. 15-00314-15-00314, 2016.

[7] T. Chen, Z. Xiaoning, B. Bai, Z. Xu, C. Wang, and W. Xia, "Numerical study of DC argon arc with axial magnetic fields," *Plasma Chemistry and Plasma Processing*, vol. 35, pp. 61-74, 2015.

[8] K. Nomura, Y. Ogino, and Y. Hirata, "Shape

control of TIG arc plasma by cusp-type magnetic field with permanent magnet," *Welding International*, vol. 26, pp. 759-764, 2012.

[9] Q. Sun, J. Wang, C. Cai, Q. Li, and J. Feng, "Optimization of magnetic arc oscillation system by using double magnetic pole to TIG narrow gap welding," *The International Journal of Advanced Manufacturing Technology*, vol. 86, pp. 761-767, 2016.

[10] H. Wu, Y. Chang, L. Lu, and J. Bai, "Review on magnetically controlled arc welding process," *The International Journal of Advanced Manufacturing Technology*, vol. 91, pp. 4263-4273, 2017.

[11] K. Nomura, Y. Ogino, T. Haga, and Y. Hirata, "Influence of magnet configurations on magnetic controlled TIG arc welding," *Transactions of JWRI*, vol. 39, pp. 209-210, 2010.

[12] M. Shoichi, M. Yukio, T. Koki, T. Yasushi, M. Yukinori, and M. Yusuke, "Study on the application for electromagnetic controlled molten pool welding process in overhead and flat position welding," *Science and Technology of Welding and Joining*, vol. 18, pp. 38-44, 2013.

[13] A. S. Baskoro, S. Frisman, A. Yogi, and W. Winarto, "Improvement of tungsten inert gas (TIG) welding penetration using the effect of electromagnetic field," in *Applied Mechanics and Materials*, 2014, pp. 558-563.

[14] M. Bachmann, V. Avilov, A. Gumenyuk, and M. Rethmeier, "About the influence of a steady magnetic field on weld pool dynamics in partial penetration high power laser beam welding of thick aluminium parts," *International Journal of Heat and Mass Transfer*, vol. 60, pp. 309-321, 2013.

[15] M. Bachmann, V. Avilov, A. Gumenyuk, and M. Rethmeier, "Experimental and numerical investigation of an electromagnetic weld pool control for laser beam welding," *Physics Procedia*, vol. 56, pp. 515-524, 2014.

[16] M. Bachmann, V. Avilov, A. Gumenyuk, and M. Rethmeier, "Experimental and numerical investigation of an electromagnetic weld pool support system for high power laser beam welding of austenitic stainless steel," *Journal of Materials Processing Technology*, vol. 214, pp. 578-591, 2014.

[17] A. V. d. Queiroz, M. T. Fernandes, L. Silva, R. Demarque, C. R. Xavier, and J. A. d. Castro, "Effects of an External Magnetic Field on the Microstructural and Mechanical Properties of the Fusion Zone in TIG Welding," *Metals*, vol. 10, p. 714, 2020.

[18] A. S. Baskoro, A. Fauzian, H. Basalamah, G. Kiswanto, and W. Winarto, "Improving weld penetration by employing of magnetic poles' configurations to an autogenous tungsten inert gas (TIG) welding," *The International Journal of Advanced Manufacturing Technology*, vol. 99, pp. 1603-1613, 2018.

[19] H. J. Aval, A. Farzadi, S. Serajzadeh, and A. Kokabi, "Theoretical and experimental study of microstructures and weld pool geometry during GTAW of 304 stainless steel," *The International Journal of Advanced Manufacturing Technology*, vol. 42, pp. 1043-1051, 2009.

[20] J. Pan, S. Hu, L. Yang, and H. Li, "Simulation and analysis of heat transfer and fluid flow characteristics of variable polarity GTAW process based on a tungsten–arc-specimen coupled model," *International Journal of Heat and Mass Transfer*, vol. 96, pp. 346-352, 2016.

[21] K. Nomura, K. Morisaki, and Y. Hirata, "Magnetic control of arc plasma and its modelling," *Welding in the World*, vol. 53, pp. R181-R187, 2009.